IEEE Access
Multidisciplinary | Rapid Review | Open Access Journal

IEEE POWER & ENERGY SOCIETY SECTION

Received April 2, 2022, accepted May 2, 2022, date of publication May 9, 2022, date of current version May 13, 2022.

Digital Object Identifier 10.1109/ACCESS.2022.3173755

Supervising Vulnerable Third Zone Distance Relay to Enhance Wide-Area Back-Up Protection Systems

BISWAJIT SAHOO[1], (Member, IEEE), SUBHRANSU RANJAN SAMANTARAY[1], (Senior Member, IEEE), AND INNOCENT KAMWA[2], (Fellow, IEEE)

[1]School of Electrical Sciences, Indian Institute of Technology Bhubaneswar, Argul, Khordha, Odisha 752050, India
[2]Department of Electrical Engineering and Computer Engineering, Faculty of Science and Engineering, Laval University, Quebec, QC G1V 0A6, Canada

Corresponding author: Subhransu Ranjan Samantaray (srs@iitbbs.ac.in)

This work was supported in part by the Canada National Sciences and Engineering Research Council (NSERC) under Grant ALLRP567550-21.

ABSTRACT Under dynamic stressed situations, distance relays are quite prone to zone-3 mal-trippings which are recognized as one of the primary causes for cascaded tripping in power systems and recent power black-outs. Our proposed algorithm enhances the zone-3 back-up protection logic by ensuring secure distance relay operation during such stressed scenarios. A parameter namely relay vulnerability index (RVI) is estimated using phasor information to rank the vulnerable relays in real time based upon the intensity of stressed conditions. Once the set of highly vulnerable relays (HVR) are recognized, an intelligent relaying logic using wide area information monitors these HVR relays. Thus, the proposed scheme effectively supervises the traditional zone-3 relay to identify fault under stressed situations. Performance analysis on IEEE 39 bus New England power system network has demonstrated high accuracy for various stressed and faulted conditions where conventional zone-3 relays mal-operate. Efficacy of the suggested scheme is validated by implementing it on RTDS platform as a part of Controller Hardware-in-Loop testing. Our proposed algorithm efficiently enhances the back-up protection operation of transmission network and significantly improves the security of distance relays without affecting the dependability.

INDEX TERMS Wide area back-up protection, relay operation margin, distance relay, phasor measurement unit, power swing, load encroachment, vulnerable relay.

I. INTRODUCTION

In current era, due to the formation of complex smartgrid network and subsequent deregulation along with growing demands, power system operates close to its rated capacity [1]. If a fault is not detected and isolated quickly, it can lead to cascaded tripping for such highly interconnected networks [2]. Distance relays are the common practice for transmission line back-up protection which gets actuated when the impedance trajectory encroaches its zone-3 operating boundary [3]. However, severe contingencies such as line outage, segregation of network, switching of large loads or generation switching can produce stressed scenarios that may lead to mal-operation of the zone-3 relay. Here, the term ''stressed scenarios'' stands for no-fault cases in which the apparent impedance drops close to the third zone operating boundary making the relay trip or at the verge of tripping. The study of recent power black-outs reveals the distance relay zone-3 mal-trippings during these dynamic stressed situations are the main reason behind cascaded failures in power systems [4]. Under such contingencies, power swing and load encroachment appears to be the main issues to consider while designing back-up protection schemes.

To overcome unwanted line tripping under these stressed conditions, various blocking schemes are implemented in distance relays [5], [6] and also an additional element namely power swing blocking (PSB) is combined with distance relay where blinder and timer are utilized to calculate the rate of variation of positive sequence impedance [7]. However, as power swings can be classified as fast or slow [8], considering the range of frequencies, the timer setting can be

The associate editor coordinating the review of this manuscript and approving it for publication was Sarasij Das.

erroneous for such variations. To detect power swings, [9] proposes a technique based on support vector machine utilizing half cycle data of current signal. However, as transient period can extend up to one cycle during any disturbance, using only half cycle window for retrieving input features may cause false tripping decision. Adaptive neuro fuzzy inference system based technique is incorporated in PSB algorithm [8]. But, its efficiency can be questionable as swing center voltage is taken as one of the input features where the threshold setting is difficult for fault cases with nearly 180° phase shift. Even though, a technique based on wavelet transform is implemented in [10], it may have reduced accuracy as wavelets are vulnerable to noisy data and needs a high sampling frequency. To mitigate third zone mal-operation under voltage instabilities, a technique in [11] utilizes voltage derivative-based parameter. But, using only rate of change of voltage is not sufficient to distinguish between voltage instability and a fault case. To deal with this disadvantage, an algorithm in [12] utilizes the variation rate of voltage and current magnitudes. But, these techniques require huge amount of off-line simulations to decide the threshold accurately.

The above-mentioned schemes use local relay information to identify faults during stressed conditions. Utilizing only local data may improve the response time of relaying operation; but has several drawbacks in case of large power system [1]. Current advancement in wide area monitoring, control and protection has utilized time-synchronised phasor measurement units (PMUs) for wide area measurement systems (WAMS). An algorithm proposed in [13] estimates apparent impedance utilizing PMU data from strategic locations to assist zone-3 operation. An adaptive technique implementing a couple of classifiers is proposed to distinguish faults and stressed scenarios [14]. As it requires PMUs to be placed at each bus to retrieve input features and needs to generate significant amount of training test cases, the algorithm becomes unfeasible for large power systems [15]. Although an effective zone-3 supervision scheme has been implemented in [16] using deep neural network based relaying protection logic, there is still a scope for improvement as the search domain can be minimized by identifying the most vulnerable relays prior to processing through data mining tool. Thus, large amount of dataset generation can be avoided which can enhance the efficacy of the scheme considering the complexity of present power network. Further, a transparent and easily implementable tool can be utilized in the relaying logic to monitor the highly vulnerable relays to detect fault cases.

Vulnerability assessment is used in literature as a valuable approach to prevent cascading failures by timely detection of the vulnerable relays that can wrongly operate in stressed situations. Thus, the objective of relay vulnerability study is to detect the set of highly vulnerable relay prone to mal-operation so as to control and monitor its operation for remedial action [16]. Relay operation margin (ROM) for the third zone which projects the distance relay vulnerability status for any operating condition, can be estimated as a function of bus voltage. In [17], operation margin analysis is carried out by calculating sensitivities of ROM to power injection. Power system security analysis is performed by measuring vulnerability index of transmission system using relay margin information. To identify the vulnerable relays (VRs), several schemes in literature have calculated the power flow from offline simulations or data received using state estimator. However, to mitigate cascaded tripping, if all the VRs are blocked, the dependability of the protection algorithm may be seriously affected. Authors in [18] have introduced two sensitivity factors based on offline analysis to determine the effect of (N − 1) contingency on the ROM and identify vulnerable relays. However, if the vulnerability analysis is performed in real time, it can update online the ranking of vulnerable relays if the system topology alters planned or unplanned. As the modern day distance relays are integrated with synchrophasor functionality, vulnerability indices can be estimated using extracted PMU information [19].

In our proposed work, an enhanced wide area distance relay protection algorithm is devised for supervision of conventional zone-3 back-up relays using real time vulnerability study (VS) and a fault detection methodology (IRL) to identify fault during stressed situations. Before the distance relays suffers any unwanted trip, a proper relay vulnerability index ought to be computed and utilized to rank the critical relays in any operational condition to estimate the intensity of vulnerability. WAMS data are retrieved from PMUs placed at strategic locations to extract the input features and compute relay operating margin and sensitivity to load power. VS detects the vulnerable relays for which the traditional zone-3 relay is blocked and IRL gets activated to discriminate fault and stressed situations. Recently developed protection logics using synchro-phasors have certain drawbacks due to failure in operation logic of distance relays, under stressed situations. Thus, the main contribution of the paper lies in

1) Enhancing the relaying decision logic by identifying the set of highly vulnerable relays (HVR) in real time and monitoring those using a transparent solution i.e. decision tree (DT) for fault detection,
2) Avoiding large amount of dataset generation as VS minimizes the search domain by detecting the HVR set prior to DT processing,
3) Validation and testing of the proposed algorithm on Controller Hardware-in-Loop (C-HIL) platform using Real Time Digital Simulator.

II. SUGGESTED ALGORITHM FOR ZONE-3 SUPERVISION

Severe stressed conditions significantly affect the zone-2 and zone-3 operations of distance relay which provides back-up protection to the transmission system. As most of the relay mal-operations are related to zone-3 of distance relay, our proposed research work is designed to serve zone-3 supervision. However, to make it more general, zone-2 supervision scheme should also be developed which may need a change in framework and analytical approach and will be considered as a part of future work.

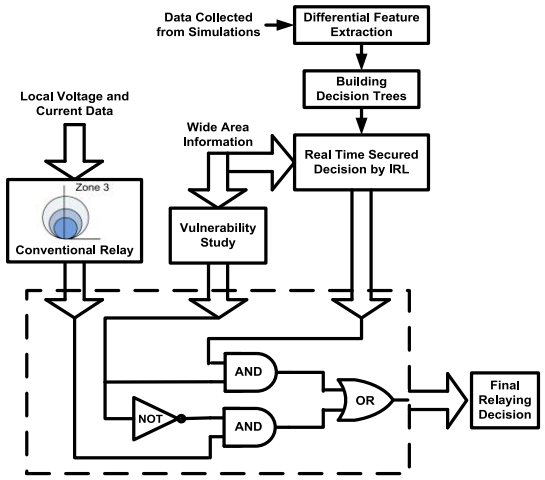

FIGURE 1. Schematic diagram of the suggested WABP scheme.

This work proposes that trip/block signal command issued by the distance relay for third zone operation during stressed conditions can be decided using the coordinated operation of conventional zone-3 and combined vulnerability study (VS) and intelligent relaying logic (IRL). Fig.1 presents the structure of the suggested algorithm for supervision of third zone relay. Initially, the Highly vulnerable relays (HVR) set is to be recognized in order to overcome relay mal-operations during stressed situations which may aggravate further and cause cascaded tripping. VS is carried out by computing a parameter termed as Relay Vulnerability Index (RVI), using wide area information. The ranking of the relays are performed according to the values of RVI. Then, for the relays which are highly vulnerable, even though the conventional zone-3 relay commands a trip, the vulnerable distance relays are blocked and do not operate. Here, IRL is activated and decides the final relaying action i.e. distinguishes between fault and stressed scenarios, instead of the traditional zone-3.

To build our decision logic IRL, a DT model is designed by feeding it with certain input features for training and testing. To extract these differential input attributes, datasets are retrieved by performing required simulation studies. Features extracted from wide area information are processed by IRL to issue real time secured decision and the datasets are classified as ''No fault/ stressed condition'' or ''Fault condition''. To classify them using DT provides excellent accuracy which makes this proposed methodology superior to existing ones. IRL produces an output of '1' for any faulted case and the distance relay trips. When IRL shows an output of '0', it is a ''no fault'' case and distance relay does not operate. Thus, the coordinated action of VS, traditional zone-3 and IRL decides for the final relaying operation.

The proposed scheme utilizes PMUs developed using Extended Kalman Filter (EKF) technique [20] for estimating phasors and subsequent retrieval of features, as the efficiency of these PMUs in estimating fundamental phasors is better compared to existing PMUs. It primarily uses a center-frequency adaptive technique, synchronized with a fundamental frequency calculated independently utilizing a demodulation technique that uses recursive discrete Fourier transform [21]. Parameters of the EKF are calibrated with respect to the calculated frequency [20]. PMU positioning strategy is incorporated as given in [22] where every line in the system should be either linked to a bus with PMU (bus_P) or remain within third zone coverage of at least two bus_P. Measurements are not accessible at rest of the buses termed as bus_N. Positive sequence voltage and current phasors for each line attached to any bus_P are collected from synchrophasors. In case of any bus_N, voltage is estimated applying the long line model of the transmission line [23]. Line parameters required in the estimation are assumed to be accessible at control centers. Calculation of the line parameters is done using the technique as proposed in [24]. Voltage phasors for any bus_N in the system are estimated by the following:

$$V_n = V_p \cosh(\gamma l) + I_p Z_c \sinh(\gamma l) \tag{1}$$

where, V_p and I_p are positive sequence voltage and current phasors respectively at bus_P, l and γ are length and propagation constant of the line respectively, Z_c = characteristic impedance.

III. VULNERABILITY STUDY

A. CONCEPT OF RELAY OPERATION MARGIN (ROM)

In case of dynamic security assessment, it is not essential to monitor all the relays placed in the power system. A set of relays which can operate for a specific power system event has to be assessed. This group of relays is termed as the vulnerable relays (VRs) and methods have to be devised to identify these. In our proposed algorithm, HVR relays out of those VRs for a specific contingency is recognized by a factor which involves the calculation of ROM. For any power system event, ROM determines the VRs which has tripped or on the verge of tripping. The after-effects of any disturbance i.e. cascaded failure, generation/load switching and separation of network, can be visualized utilizing ROM value.

For third zone of distance relay, a mho relay characteristic is chosen for analysis and subsequent study. For any line i-j, the relay operation margin for relay ij (ROM_{ij}) is calculated as

$$ROM_{ij} = \left|Z_{ijc}\right| - \rho_{ij} \tag{2}$$

where Z_{ijc} is the apparent impedance with respect to centre of third zone and ρ_{ij} is the radius of third zone. If Z_{ij} is the impedance seen by the relay measured from the origin and R_{ijc} and X_{ijc} are x-y co-ordinates of center of zone-3 boundary, ROM_{ij} can be given by

$$ROM_{ij} = \left|Z_{ij} - \left(R_{ijc} + jX_{ijc}\right)\right| - \rho_{ij} \tag{3}$$

Under normal operational scenario, the apparent impedance seen by the relay stays out of the operational zone and ROM_{ij} has a positive value. If the apparent impedance encroaches into the operating boundary, ROM_{ij} is negative and the distance relay commands a trip decision. This apparent

impedance sensed by the distance relay depends on the complex power flow in the line along with magnitude and the power factor of the load impedance. If V_i and V_j are the magnitudes and θ_{ij} denotes phase angle difference of line voltages at both line ends, then complex power flow in the line i-j, S_{ij} is given by:

$$S_{ij} = \frac{\sqrt{\left(V_i^2 - V_i V_j \cos\theta_{ij}\right)^2 + \left(V_i V_j \sin\theta_{ij}\right)^2}}{Z_{ij}} \tag{4}$$

If Z_{Lij} be the line impedance between node i and j, then Z_{ij}, the apparent impedance seen by the relay under any operating condition (fault or no-fault) is expressed as:

$$|Z_{ij}| = \frac{V_i^2}{S_{ij}} = \frac{Z_{Lij} V_i}{\sqrt{(V_i - V_j \cos\theta_{ij})^2 + (V_j \sin\theta_{ij})^2}} \tag{5}$$

B. SENSITIVITIES OF RELAY OPERATION MARGIN TO BUS VOLTAGES

As ROM depends upon bus voltage, it changes with variation in voltage under any abnormal system event. The sensitivity study can determine the rate of change in operating margin trajectory i.e. the change in ROM with respect to change in bus voltages or load power injection. Hence, it can be used as an index to determine vulnerability of a distance relay under any contingency.

The sensitivity of relay operation margin with respect to load power at a particular operating point is given by

$$\Delta ROM = \begin{bmatrix} S_{RP} & S_{RQ} \end{bmatrix} \begin{bmatrix} \Delta P \\ \Delta Q \end{bmatrix} \tag{6}$$

where ΔP and ΔQ are the change in active and reactive power, respectively. S_{RP}, S_{RQ} are the sensitivity of relay operation margin with respect to active and reactive power respectively. These can be expressed in terms of change in bus voltages (both angle and magnitude) using a jacobian matrix M as

$$\begin{bmatrix} \Delta P \\ \Delta Q \end{bmatrix} = M \begin{bmatrix} \Delta\theta \\ \Delta V \end{bmatrix} = \begin{bmatrix} \frac{\partial \Delta P}{\partial \theta} & \frac{\partial \Delta P}{\partial V} \\ \frac{\partial \Delta Q}{\partial \theta} & \frac{\partial \Delta Q}{\partial V} \end{bmatrix} \begin{bmatrix} \Delta\theta \\ \Delta V \end{bmatrix} \tag{7}$$

If $S_{R\theta}$ and S_{RV} are the sensitivity of relay operation margin with respect to bus voltage angle and magnitude, respectively, it can be related to ΔROM using the following expression:

$$\Delta ROM = \begin{bmatrix} S_{R\theta} & S_{RV} \end{bmatrix} \begin{bmatrix} \Delta\theta \\ \Delta V \end{bmatrix} \tag{8}$$

Thus, by putting (7) in (6) and comparing with (8),

$$\begin{bmatrix} S_{RP} & S_{RQ} \end{bmatrix} = \begin{bmatrix} S_{R\theta} & S_{RV} \end{bmatrix} M^{-1} \tag{9}$$

For any line-ij, sensitivity parameters with respect to line end voltages (θ_i, θ_j, V_i, V_j) can also be expressed by

$$\begin{bmatrix} S_{R\theta} & S_{RV} \end{bmatrix} = \begin{bmatrix} \frac{\partial ROM_{ij}}{\partial \theta_i} & \frac{\partial ROM_{ij}}{\partial \theta_j} & \frac{\partial ROM_{ij}}{\partial V_i} & \frac{\partial ROM_{ij}}{\partial V_j} \end{bmatrix} \tag{10}$$

Sensitivities of ROM with respect to any variable 'y' is derived in terms of the apparent impedance seen by the relay Z_{ij} and the load angle $\emptyset_{ij}$ and given as the following:

$$\frac{\partial ROM_{ij}}{\partial y} = \left[\frac{a\cos\varphi_{ij} + b\sin\varphi_{ij}}{c}\right] \frac{\partial Z_{ij}}{\partial y} \tag{11}$$

where $a = Z_{ij}\cos\emptyset_{ij} - R_{ijc}$, $b = Z_{ij}\sin\emptyset_{ij} - X_{ijc}$ and $c = \sqrt{a^2 + b^2}$. The expression for $\frac{\partial Z_{ij}}{\partial y}$ taking y as θ_i, θ_j, V_i, V_j respectively, are derived and presented in the equations (12)-(15). These can be put in (11) to obtain sensitivity parameters with respect to line end voltages which can be used further to calculate relay vulnerability index as given in section III (C).

$$\frac{\partial Z_{ij}}{\partial V_i} = \frac{Z_{ij}(k - V_i(V_i - V_j\cos\theta_{ij}))}{k^{1.5}} \tag{12}$$

$$\frac{\partial Z_{ij}}{\partial V_j} = \frac{Z_{ij} V_i (V_i\cos\theta_{ij} - V_j)}{k^{1.5}} \tag{13}$$

$$\frac{\partial Z_{ij}}{\partial \theta_i} = \frac{-Z_{ij} V_i^2 V_j \sin\theta_{ij}}{k^{1.5}} \tag{14}$$

$$\frac{\partial Z_{ij}}{\partial \theta_j} = \frac{Z_{ij} V_i^2 V_j \sin\theta_{ij}}{k^{1.5}} \tag{15}$$

where

$$k = (V_i - V_j\cos\theta_{ij})^2 + (V_j\sin\theta_{ij})^2 \tag{16}$$

C. RELAY VULNERABILITY INDEX

As mentioned earlier, under any dynamic stressed condition such as power swing and load encroachment, relay operation margin decreases and sensitivities of relay operation margin to bus voltages increase. By combining these two parameters, a factor named as Relay Vulnerability Index (RVI) is computed to rank the relays according to the severity of vulnerable zone-3 and determine the set of highly vulnerable relays (HVR). It can be computed as the ratio of the relay operation margin (presented in (4)) and sensitivity of relay operation margin (presented in (8)) and is given by the following:

$$RVI_{ij} = \frac{ROM_{ij}}{\Delta ROM_{ij}} \tag{17}$$

Using wide area information, RVI is calculated for each relay in the system under different dynamic events. It can identify the most vulnerable zone-3 relays on the verge of mal-operation during stressed situations at a given operating point. The relays having negative or lower value of ROM and large Δ ROM produce negative or small RVI and are included in HVR.

IV. FORMULATION OF INTELLIGENT RELAYING LOGIC (IRL)

To identify faults during dynamic stressed situations is quite a challenging topic of research. Our proposed algorithm suggests during certain operating scenarios where conventional zone-3 mal-trips, if it can be blocked prior and decision-making can be shifted to an improved decision logic, the reliability of protection relays can be improved substantially.

Thus, to enhance distance relay operation, a decision logic is devised employing decision tree (DT) which is designed to distinguish between fault and stressed situations.

A. THEORETICAL BACKGROUND

A DT basically consists of certain simple and exact rules applying if–then statements which classify the datasets considering its unique features [25]. DT model has to be trained using sufficient amount of relevant datasets having predefined classes for every dataset. Certain comparison rules are imposed to segregate the data into a number of subsets. Each of the variables is used in the search to split the datasets and the data having maximum amount of similarity are clustered.

DT is created by building a tree with training dataset as long as the terminating nodes acquire the samples of a single class. The splitting rule is followed to construct classification tree. Among various splitting mechanism employed for classification, Gini splitting rule is popular. It involves a function namely impurity function [25] I(m) for node m, and can be given by

$$I\,(m) = -\sum_{i=1}^{k} p\,(w_i|m)\log p(w_i|m) \tag{18}$$

where $p\,(w_i|m)$ is the portion of samples allotted to class w_i at node m and k, l=1, …, k is the index of class. Again, impurity function for Gini splitting rule can be presented as follows:

$$I\,(m) = \sum_{n=1}^{j} p\,(j\,|\,m)\,p\,(n\,|\,m), \quad j \neq 1 \tag{19}$$

where n=1, …, j, j denotes the index of class and $p\,(j\,|\,m)$ stands for the conditional probability of class j at node m. Gini splitting rule finds out the biggest class among training datasets and separate it out from other sets. Once the decision trees are created, the correct tree has to be selected next for classification.

Various levels and sub-trees are associated with the decision trees. Optimal simpler tree is decided by removing less relevant nodes and sub-trees known as tree pruning method. Minimum error pruning technique is employed here. The resubstitution errors and cross-validation errors calculate the training dataset accuracies. These errors reduce when the tree size increases, however after a certain limit, with the tree size, the cross-validation error rate starts increasing. So, the practice is to select the tree having minimum cross-validation error. Once the training is done, the dataset kept for testing are utilized to test the trained model. The superiority of decision tree is that it requires less time for training in comparison with other data mining tools whatever be the dataset complexity. Even when large data samples are taken, it requires only a few seconds for training with good accuracy level.

B. SELECTION OF INPUT ATTRIBUTES

To develop a DT structure, suitable input features should be selected and fed to the model. Selection of these attributes is done considering the unique nature of various power system contingencies like fault, power swings or load encroachment.

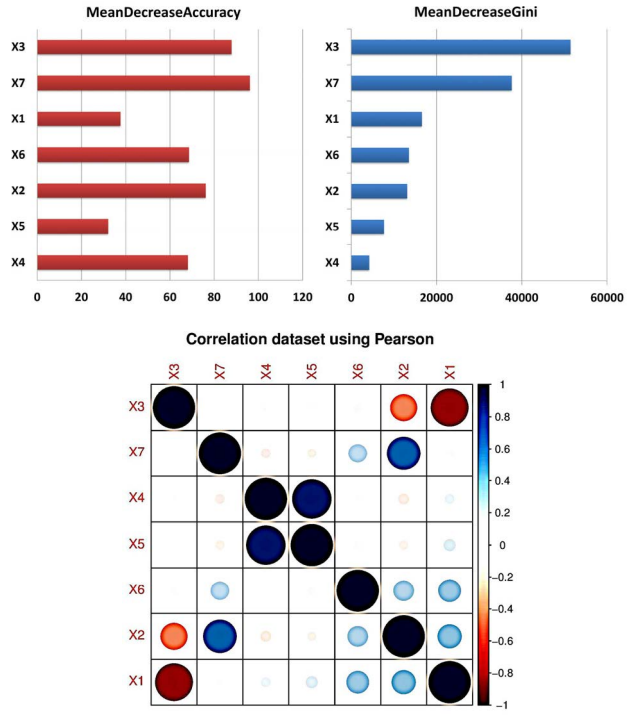

FIGURE 2. Analysis of input dataset (a) Mean decrease accuracy plot (b) Mean decrease gini plot (c) Correlation among the input dataset.

Use of just positive sequence voltage phasor information is not adequate to separate stressed situations from symmetrical fault as their characteristics are often similar. Hence, some additional features i.e. active and reactive power and their derivatives are computed and given as inputs to improve the accuracy level. The input features for our decision tree model are described as below:

1) X1: ΔV = Change in voltage magnitude (Positive sequence), 2) X2: $\Delta\delta$ = Change in voltage phase angle (Positive sequence), 3) X3: ΔI = Change in current magnitude (Positive sequence), 4) X4: ΔP = Variation in active power 5) X5: ΔQ = Variation in reactive power, 6) X6: $\frac{dP}{dt}$ = Variation rate of active power, 7) X7: $\frac{dQ}{dt}$ = Variation rate of reactive power. Any differential feature ΔIF is estimated as:

$$\Delta\mathrm{IF(w)} = \Delta\mathrm{X_i(w)} - \Delta\mathrm{X_j(w)} \tag{20}$$

Here 'w' is the sample count. ΔIF denotes differential attribute for line linking bus 'i' and 'j'. $\mathrm{X_i(w)}$ is the measurement at bus "i" for $\mathrm{w^{th}}$ sample, $\Delta\mathrm{X_i}$ denotes the difference of consecutive samples at bus 'i'. This single end change for $\mathrm{w^{th}}$ sample at bus 'i', $\Delta\mathrm{X_i(w)}$ is given as follows:

$$\Delta\mathrm{X_p(w)} = \mathrm{X_p(w)} - \mathrm{X_p(w-1)} \tag{21}$$

The relative importance of different features is analyzed using mean decrease accuracy and mean decrease Gini plots. These plots are presented in Fig. 2(a) and (b), for a particular relay (i.e. in this case R29-28, relay placed on bus 29 for line 29-28, as shown Fig.5). Though seven features are used as inputs to train the model, only three of those i.e. x3, x6 and x7, (ΔI, dP/dt and dQ/dt) can be denoted as the most

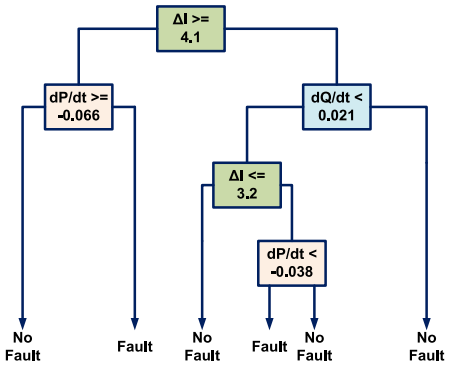

FIGURE 3. Constructed DT model for fault identification on IEEE 39-bus system (R29-28).

dominant features. Fig. 2(a) depicts the weight of individual features by specifying the decrease in accuracy on ignoring that feature from the input set taken to train the model. A correlation plot as presented in Fig. 2(c) indicates the degree of correlation between the pair of variables. The correlation plot clearly shows that x7 is highly correlated to x2 i.e. $\Delta\delta$ and x3 is highly correlated to x1 i.e. ΔV and thus, those can be pruned from the DT structure without affecting the accuracy significantly. From the variable importance plots and the DT structure as given in Fig. 3, it is clear that x7, i.e. dQ/dt and x3, i.e. ΔI are the most significant input features. Thus, ΔI in the line is the primary feature that differentiates fault from no-fault while dP/dt and dQ/dt features further enhance the resolution for classifying faults from power swings, voltage instabilities and load encroachment scenario which justifies the fundamental principles defined for such contingencies.

C. SCHEMATA OF THE PROPOSED INTELLIGENT RELAYING LOGIC (IRL)

Voltage and current measurements collected at the relay are processed by PMUs to extract fundamental positive sequence phasor information. To form the dataset required for classifying fault and no-fault or stressed situations, initially, change in signals at a single end (ΔV, ΔI, $\Delta\delta$, ΔP and ΔQ) are computed. Using these single-ended features, differential changes from both line ends are calculated. During offline studies, the DT model is trained for classification of fault and stressed scenario. During online processing, wide area information is utilized to extract the input features and fed to the trained DT model (IRL logic) for final relaying decision. A fault is detected when IRL issues an output of '1' and trip command is sent to the distance relay. When IRL provides an output of '0', a no-fault situation is detected and no tripping signal is issued. The traditional zone-3 relay is always controlled by the command issued by VS. The flowchart of the suggested algorithm is shown in Fig.4.

V. RESULT ANALYSIS AND DISCUSSION

The suggested WABP scheme is tested on IEEE 39 bus New England system as presented in Fig. 5 using

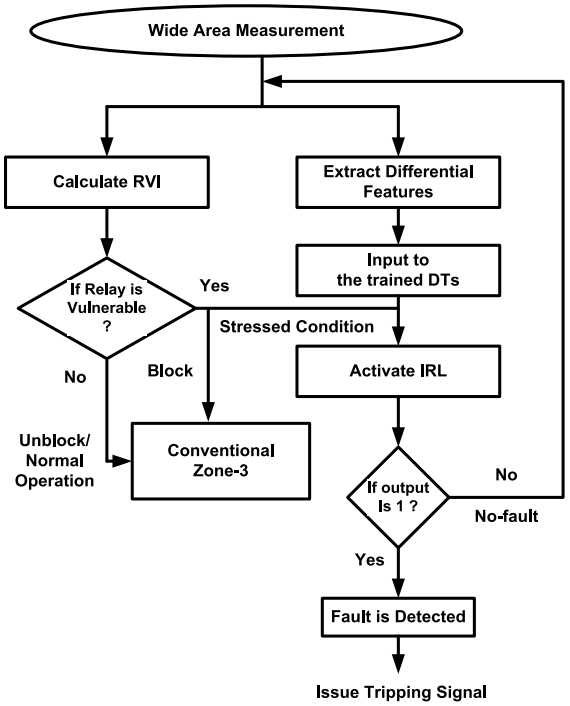

FIGURE 4. Flowchart of the suggested algorithm.

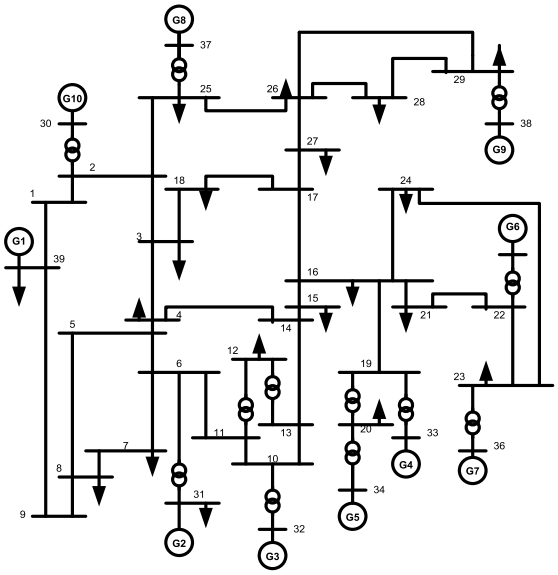

FIGURE 5. Single diagram of IEEE 39-bus new england system.

MATLAB/Simulink platform. Following the PMU placement criteria, PMUs are placed at bus 4, 7, 9, 10, 11, 15, 18, 19, 22, 24, 25, 27, 29 and 34 respectively as shown in Fig. 5. Extensive simulations are performed to collect dataset for testing and training IRL decision logic. DT model is constructed using Rattle [26] Software, utilizing the extracted data from offline simulations. Trained DT structures are used to implement IRL which issues correct tripping decision in real time. As the training dataset is produced from several

TABLE 1. RVI index: power swing scenario.

For fault duration of 0.12s			
Relay	ROM	RVI	Rank
R29-28	-0.1773	-0.1484	1
R26-25	0.1925	0.1723	2
R26-27	0.4326	0.2673	3
R26-28	0.6823	0.4862	4
R17-27	0.7526	0.5343	5

TABLE 2. RVI index: load encroachment scenario.

Case : Load = 196.7% of base load			
Relay	ROM	RVI	Rank
R29-28	-0.0099	-0.0056	1
R25-26	-0.0118	-0.0061	2
R28-26	0.1056	0.0762	3
R26-25	0.1296	0.0956	4
R26-28	0.2216	0.1068	5
R26-29	0.2486	0.1224	6
R29-26	0.2512	0.1256	7
R28-29	0.2950	0.1568	8
R25-2	0.3356	0.1768	9
R2-25	0.3648	0.1856	10

time-series simulations on the given test system, adequate data from post-fault dynamics should be collected to train the DT model. Training datasets should contain sufficient data to decide the threshold for correct classification for each operating scenario.

A. PERFORMANCE OF VULNERABILITY STUDY (VS)

Consider a case of three phase fault produced on line 29-26 sustaining for certain time duration and cleared afterwards by opening of CB. The HVR set have negative or very small positive values of RVI. The relays that may encounter power swings are ranked based on the RVI values, in Table 1. For certain relays, RVI index has a negative value. Thus, the apparent impedance encroaches into third zone and can cause maloperation. For a few relays, RVI values are positive and very small. Thus, these relays can be at the verge of tripping. The VS stage identifies these cases as stressed situation, block the conventional zone-3 and direct the decision switch to IRL.

To produce a load encroachment scenario, initially, line 26-27 is disconnected from the network. Then, when the loads at bus 28 and 26 are raised in steps from 100% to 250%, at a particular condition, the apparent impedance seen by the distance relay can encroach its third zone boundary and may result into mal-tripping of relay R29-28 and R25-26. The relays having negative or very small positive RVI values can be termed as highly vulnerable. Table 2 shows the relay ranking sorted according to RVI values or the severity of vulnerability for this case.

B. PERFORMANCE STUDY OF IRL LOGIC

1) DATASET GENERATION FOR TRAINING AND TESTING

Datasets are collected from extensive simulation under different operating points and system events on the test system. Dataset for fault cases are collected from simulation of various unsymmetrical faults (SL-G, LL-G, L-L) and symmetrical faults (LLL) at 10 various fault locations (5% to 95%) with 5 values of fault resistance (0.01, 1, 10, 50, 100Ω). Current and voltage measurement at different relays are sent for processing to extract input attributes for DT model. It is observed, differential attributes provides higher prediction accuracy compared to single-ended ones. For collecting dataset for power swing cases, a LLL fault is produced on line 29-26, and circuit breaker is opened after 5 to 12 cycles. Following the line clearance, a power swing occurs at R29-28 and the apparent impedance encroaches into its third zone. A load encroachment case is produced by raising load at bus-28 and bus-26 following a line outage on line 27-17. Under this scenario, voltage dip is seen at bus 29 and reactive power loss in line 29–28 rises. Further, the apparent impedance encroaches into zone-3 of R29-28. Datasets for no-fault condition covers the normal system operational condition cases as well as external fault cases where apparent impedance does not cross the critical boundary to be announced as stressed situation i.e faults on line 27-17, 25-2 for R29-28.

2) TRAINING AND TESTING OF IRL LOGIC

Training and testing of DT model is done using the collected datasets with 70:30 ratio. From empirical studies, it is obtained that if the datasets are divided with 70% for training and 30% for testing, the efficiency is quite high for various system configurations and operating scenarios. Table 3 presents the fault detection accuracies for IRL logic at different relays of test system, during training and testing period. During training, the fault detection accuracy is around 99.46% whereas the trained DT model provides overall 99.38% prediction accuracy for actual fault and no-fault cases. Table 4 presents the confusion matrix created after testing which shows prediction accuracy for relay R29-28. Only 9 no-fault cases are incorrectly predicted as fault whereas 5 actual fault cases are mis-classified as no-fault. Thus, fault and stressed cases are classified with high accuracy.

TABLE 3. Prediction accuracy of IRL logic at different relays.

Relay	Fault Detection Accuracy		
	Training	Testing	Testing (with 20dB SNR)
R29-28	99.52	99.44	99.4
R29-26	99.56	99.46	99.38
R27-28	99.6	99.52	99.44
R27-17	99.44	99.36	99.32
R25-26	99.52	99.46	99.42
R25-2	99.12	99.04	98.98

To examine the robustness of the suggested algorithm to measurement noise i.e. error in PMU measurement, noise is added to the magnitude and phase angle measurements. Gaussian white noise having signal-to-noise ratio (SNR) of 20 dB is added to the test data and the trained DT model is tested by feeding that noisy input. The fault detection accuracies for IRL logic, with measurement noise at different relays of

TABLE 4. Confusion matrix generated after testing at R29-28.

		Actual Class	
		NF	F
Predicted Class	NF	1496	5
	F	9	995
Prediction Accuracy		99.4	99.5

TABLE 5. Performance of the suggested algorithm during various contingencies.

Cases	VS Output	Zone-3 at bus 29-28	IRL Output	Final Decision
Three Phase Fault	0	1	Not Triggered	1
Voltage Instability	1	1 (Blocked)	0	0
Power Swing	1	1 (Blocked)	0	0
Fault Under Power Swing	1	1 (Blocked)	1	1

the test system are presented in Table 3. Interestingly, the testing accuracies show our model is immune to noise. For various fault locations, fault resistances, fault types, different faulted lines, and for varied fault clearing instants for powers swing, the fault and no-fault conditions can be predicted with reasonable efficiency.

C. PERFORMANCE UNDER VARIOUS OPERATING SCENARIOS

The performance of our suggested methodology is validated for different system operating scenarios where the impedance trajectory seen by the distance relay encroaches its third zone, and the result analysis is presented in Table 5.

During a LLL fault at 75% of line 28-26, the impedance trajectory at the relay enters into third zone of R29-28 as presented in Fig. 6(a). Before the fault inception, the system state is normal, thus VS stage issues an output of '0' as presented in first row of Table 5 and assigns the relay as not vulnerable. In this case, the decision-making remains with conventional zone-3 relay that detects the occurrence of fault and trip command is initiated. To observe the performance during voltage instability, the reactive powers at bus 15, 16 and 21 are multiplied so that the voltage at bus 16 drops by 36.5% and the impedance trajectory encroaches its zone-3 as presented in Fig. 6(b). For this voltage stressed condition, VS assigns the relay as vulnerable. Block command is sent for the conventional zone-3 relay and IRL gets actuated. As IRL detects the situation as stressed or no-fault, there is no tripping signal for the distance relay as presented in Table 5.

To observe the performance under power swing, a LLL fault is created on line 29-26 at 3.0s with CB opening at 3.16s. A power swing is seen at relay R29-28 and the apparent impedance encroaches its zone-3 as presented in Fig.6(c). For this case, the suggested algorithm operated just like the voltage instability scenario, given in Table 5. If a fault occurs

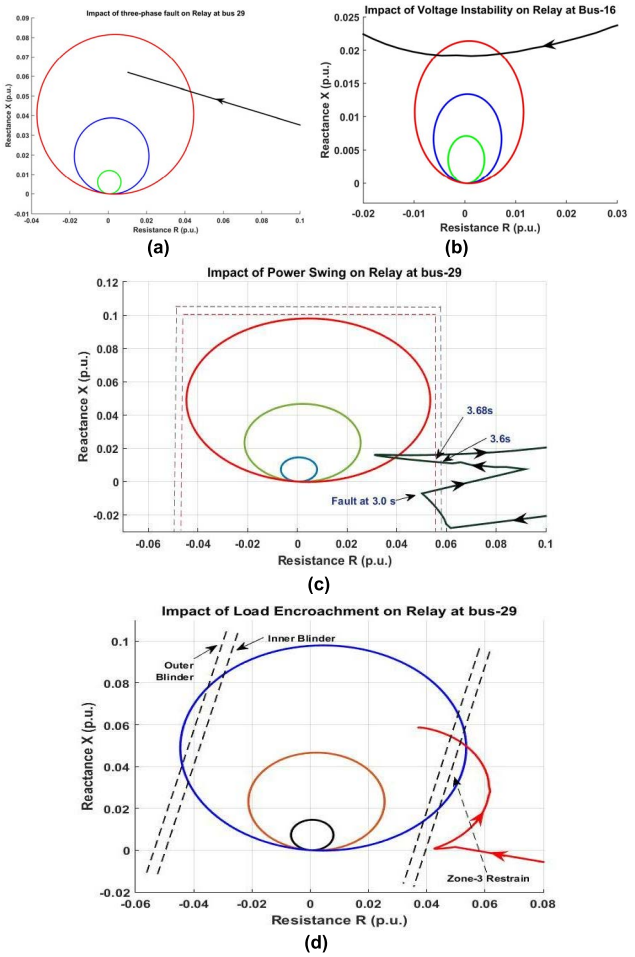

FIGURE 6. Impedance trajectory for Various System Events (a) Three phase zone-3 fault (b) Voltage Instability (for a voltage dip of 36.7%) (c) Power swing (d) Load Encroachment at 196.7% load.

under this power swing scenario (as presented in last row of Table 5), the tripping decision is issued by IRL logic as VS blocks the conventional zone-3 relay. IRL produces the output as ''1'' detecting it as a fault condition and sends a tripping signal. To create a load encroachment case, the loads at bus 26 and 28 are increased by 196.7% step by step and the apparent impedance of each relay is observed. The R-X trajectory for relay R29-28 is found to encroach its zone-3 as presented in Fig. 6(d). Under this scenario, proposed scheme blocks the conventional zone-3 relay and activates IRL for final relaying decision i.e. no-trip signal.

For a case of stable power swing (SPS), after certain duration, the power flow in the line becomes nearly stable. However, the relay may face large oscillations in current and voltage during severe angular instability. If fault clearing time is high, there can be unstable oscillations and the generators may face an out-of-step. This unstable power swing (UPS) situation can create unintentional islanding and loss of system stability. To predict UPS and separate SPS and UPS cases is a challenging subject for researchers and can come under the scope of future work.

TABLE 6. Comparison with existing schemes (IEEE 39-bus system).

Relay	Stressed Cases (Actual: 480)		Fault Cases (Actual: 12000)	
	Predicted	Accuracy	Predicted	Accuracy
Conventional blinder	275	57.29	-	-
SVM	387	80.62	9664	80.53
ANN	394	82.08	9760	81.33
Proposed Scheme	476	99.16	11885	99.04

D. COMPARATIVE ANALYSIS WITH EXISTING METHODS

The efficacy of the algorithm is exhibited here in comparison with traditional blinder techniques. In traditional schemes, two concentric polygons blinders are employed to detect power swing [7], and load blinder [27] is implemented to block third zone operation for load encroachment. For concentric polygons blinders, inner blinder is placed in the outer region of third zone protection boundary. Outer blinder is set with resistive reach of 5% security margin of estimated maximum load and reactive reach of 20% margin of maximum mho relay reach. The slip frequency is considered to be maximum of 2Hz and the minimum blocking duration is taken to be 10ms [7].

For certain power swing cases, the concentric blinders fail to recognize the swing due to very high impedance variation rate during disturbance period. After fault removal, R-X trajectory as presented in Fig.6(c) encroaches into the outer blinder at 3.61s and inner blinder at 3.69s. The above situation can be wrongly classified as out-of-step. Similarly, for a load encroachment case, as the impedance trajectory seen by R29-28 encroaches into the traditional load blinder, it cannot avoid third zone maloperation as shown in Fig. 6(d).

Total of 480 stressed cases (288 scenarios of power swing and 192 scenarios of load encroachment) where distance relay mal-trips, are tested and the efficacy of various schemes are presented. The proposed scheme can avert 476 scenarios of mal-tripping. Traditional zone-3 relay declare all of the stable swing scenarios as faulted situation whereas IRL claimed 286 scenarios to be no-fault (2 cases of maloperation). Applying concentric polygon blinder setting, just 177 scenarios of third zone false-trippings are prevented. In case of load encroachment, 190 out of 192 simulated cases are found to be no-fault situation by IRL and load blinder prevented just 98 cases of third zone mal-trippings.

The performance of IRL is also compared with other data-mining algorithms, like support vector machine (SVM), neural network (NN). The estimation accuracies for these existing techniques are shown in Table 6 for the test system. We can see that the algorithms using tools like SVM and NN give high prediction error. The prediction accuracies comes in the ranges of 80-83% in identifying the fault.

E. RESPONSE TIME FOR THE SUGGESTED ALGORITHM

It is observed, the total average time needed to extract online differential features from phasor measurement data and decision by VS and IRL is within 6-10ms. Therefore, average time required by the controller algorithm to generate the corresponding output is less than half cycle. But, the total delay comprising of processing, multiplexing of phasor information (taking 10-12 cycles of measurement) as well as the transducers can be around 75 ms [28]. In addition, the employment of fiber optics communication channel can add a delay of around 25 ms which is an approximate value for specific system features such as system size, communication apparatus [28]. So, an overall delay should be around 100-110ms. As the average detection time for the most vulnerable relays falls in the range of 115-125 ms, it renders adequate time to activate suitable remedial techniques. Thus, if common timer setting for zone-3 operation is considered to be 1000-2000ms (50Hz system) [1], the response time of the devised algorithm does not create any problem. Thus, it is inferred that the proposed algorithm can be incorporated in real time.

VI. HARDWARE IMPLEMENTATION ON REAL TIME DIGITAL SIMULATOR (RTDS) PLATFORM

For validating the efficacy of the suggested algorithm, the discussed scheme is implemented on RTDS platform [29] as a part of Controller hardware-in-the-loop (CHIL) testing. TESLA 4000 hardware PMUs (provided by ERL) are installed in the laboratory. To incorporate a low-level interface-based CHIL testing, a floating point digital-signal processor (DSP) TMS320C6713 is implemented. For the CHIL testing, the proposed algorithm is incorporated on the DSP board via Code Composer Studio and this DSP-based controller is the hardware to be tested. As interfacing is accomplished with low level signal that varies between +/−10 V and <50 mA, no extra interfacing tool is needed for C-HIL testing.

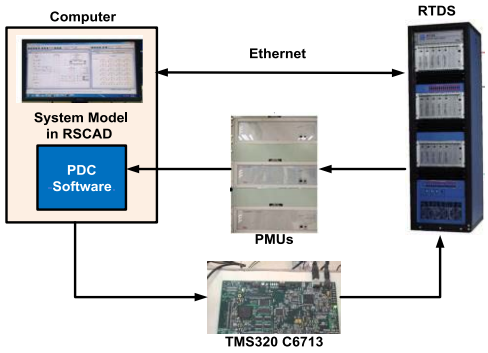

FIGURE 7. Lab Set-up for C-HIL testing of the suggested algorithm.

The gigabit transceiver analog output (GTAO)/ digital input (GTDI) card of RTDS are utilized for interfacing between the external controller, hardware PMUs, and the system model in RSCAD. Fig. 7 presents the devices used and the developed laboratory set-up. The C-HIL testing is performed using WSCC-9 bus system model [30]. The three phase instantaneous voltage and current signals from bus 7, 9 and 4 are collected from 18 analog output channels of RTDS

TABLE 7. C-HIL test results on RTDS platform.

	Test Cases	Trip (1)/ No-trip (0)	Time of Operation (ms)
Stressed Conditions	Stable Power Swing on Line 7-8	0	-
	Load Encroachment on Line 7-8	0	-
	Voltage Instability on Line 4-6	0	-
Line Faults Under Stressed Conditions	LLL fault on line 4-6	1	116.5
	L-G fault on line 7-5	1	117.4
	L-L fault on line 7-8	1	116.9

hardware interface GTAO card and fed to the PMUs. Thus, three hardware PMUs are connected at bus 7, 9 and 4 and supply C37.118 complied coded data (phasor information) to ePDC (phasor data concentrator) which is subsequently decoded and the retrieved feature information is fed to the digital-signal processor. The trip command from the controller is sent to the concerned circuit breakers of the test system using GTDI card. Table 7 presents the performance of the scheme under C-HIL testing with response time for fault detection. Considering a total delay comprising of processing, multiplexing of phasor information, PDC data extraction to be 100-110 ms and response time of the controller to command tripping signal to be 10-15 ms, the average fault detection time for the most vulnerable relays falls in the range of 115-125 ms, as reflected in Table 7. It can be inferred from the results that the suggested scheme is capable of discriminating stressed situations from faulted scenarios accurately with better response time.

VII. CONCLUSION

As the conventional zone-3 algorithms are susceptible to mal-operation under stressed conditions like power swing, load encroachment and voltage instability, there is a necessity of zone-3 supervision to enhance the security of protection operation. Our proposed scheme defines a factor, Relay Vulnerability Index which is used to rank the highly vulnerable relays during any disturbance period. This vulnerability study logic issues a blocking signal for the third zone of highly vulnerable relays. Further, it switches the operation from conventional zone-3 relay to an intelligent relaying logic that uses wide area information for real time secured decision. Relevant simulations are performed to extract input differential attributes for training of the decision tree model that distinguishes fault from stressed situations. The result analysis on IEEE 39-bus New England system demonstrates excellent performance under different operating conditions where conventional zone-3 mal-trips. C-HIL testing on RTDS platform demonstrates high efficacy of the suggested algorithm in real time scenario. Thus, our proposed scheme can avoid relay mal-operations that may initiate cascading failure and enhance the security aspect of zone-3 protection.

REFERENCES

[1] S. H. Horowitz and A. G. Phadke, "Third zone revisited," *IEEE Trans. Power Del.*, vol. 21, no. 1, pp. 23–29, Jan. 2006.

[2] *Final Report on the August 14, 2003 Blackout in the United States and Canada: Causes and Recommendations*. [Online]. Available: https://www.energy.gov/oe/downloads/blackout-2003-final-report-august-14-2003-blackout-united-states-and-canada-causes-and, https://www.energy.gov/

[3] S. H. Horowitz and A. G. Phadke, *Power System Relaying*, 3rd ed. Hoboken, NJ, USA: Wiley, 2008.

[4] V. Madani, D. Novosel, S. Horowitz, M. Adamiak, J. Amantegui, D. Karlsson, S. Imai, and A. Apostolov, "IEEE PSRC report on global industry experiences with system integrity protection schemes (SIPS)," *IEEE Trans. Power Del.*, vol. 25, no. 4, pp. 2143–2155, Oct. 2010.

[5] C. Pang and M. Kezunovic, "Fast distance relay scheme for detecting symmetrical fault during power swing," *IEEE Trans. Power Del.*, vol. 25, no. 4, pp. 2205–2212, Oct. 2010.

[6] J. Blumschein, Y. Yelgin, and M. Kereit, "Proper detection and treatment of power swing to reduce the risk of blackouts," in *Proc. 3rd Int. Conf. Electric Utility Deregulation Restructuring Power Technol.*, Apr. 2008, pp. 2440–2446, doi: 10.1109/DRPT.2008.4523821.

[7] (2005). *IEEE Power System Relay Committee Working Group D6: Power Swing and Out-of-Step Considerations on Transmission Line*. [Online]. Available: http://www.pes-psrc.org/Reports/PowerSwing and OOS Considerations on Transmission Lines F.pdf

[8] K. Seethalekshmi, S. N. Singh, and S. C. Srivastava, "A classification approach using support vector machines to prevent distance relay maloperation under power swing and voltage instability," *IEEE Trans. Power Del.*, vol. 27, no. 3, pp. 1124–1133, Jul. 2012.

[9] N. G. Chothani, B. R. Bhalja, and U. B. Parikh, "New support vector machine-based digital relaying scheme for discrimination between power swing and fault," *IET Gener., Transmiss. Distrib.*, vol. 8, no. 1, pp. 17–25, Jan. 2014.

[10] S. M. Brahma, "Distance relay with out-of-step blocking function using wavelet transform," *IEEE Trans. Power Del.*, vol. 22, no. 3, pp. 1360–1366, Jul. 2007.

[11] M. Jonsson and J. E. Daalder, "An adaptive scheme to prevent undesirable distance protection operation during voltage instability," *IEEE Trans. Power Del.*, vol. 18, no. 4, pp. 1174–1180, Oct. 2003.

[12] M. Sharifzadeh, H. Lesani, and M. Sanaye-Pasand, "A new algorithm to stabilize distance relay operation during voltage-degraded conditions," *IEEE Trans. Power Del.*, vol. 29, no. 4, pp. 1639–1647, Aug. 2014.

[13] P. Kundu and A. K. Pradhan, "Synchrophasor-assisted zone 3 operation," *IEEE Trans. Power Del.*, vol. 29, no. 2, pp. 660–667, Apr. 2014.

[14] S. Das, R. Dubey, and B. K. Panigrahi, "Secured zone-3 protection during power swing and voltage instability: An online approach," *IET Gener. Transm. Distrib.*, vol. 11, no. 2, pp. 437–446, 2017.

[15] B. Sahoo, S. R. Samantaray, and B. R. Bhalja, "An effective zone-3 supervision of distance relay for enhancing wide area back-up protection of transmission system," *IEEE Trans. Power Del.*, vol. 36, no. 5, pp. 3204–3213, Oct. 2021.

[16] Z. Liu, Z. Chen, and Y. Hu, "Detection of vulnerable relays and sensitive controllers under cascading events based on performance indices," in *Proc. Power Energy Soc. Gen. Meeting*, Jul. 2014, pp. 1–5.

[17] S. H. Li, N. Yorino, and Y. Zoka, "Operation margin analysis of zone 3 impedance relay based on sensitivities to power injection," *IET Genr. Transm. Distrib.*, vol. 1, no. 2, pp. 312–317, 2007.

[18] M. K. Jena and B. K. Panigrahi, "Event-triggered vulnerable relay identification and supervision to prevent zone-3 mal-operations," *IEEE Syst. J.*, vol. 13, no. 3, pp. 3368–3375, Sep. 2019.

[19] North American SynchroPhasor Initiative. (2019). *Vulnerability Analysis of Distance Relays using PMU Data*. [Online]. Available: http://www.naspi.org

[20] I. Kamwa, S. R. Samantaray, and G. Joos, "Compliance analysis of PMU algorithms and devices for wide-area stabilizing control of large power systems," *IEEE Trans. Power Syst.*, vol. 28, no. 2, pp. 1766–1778, May 2013.

[21] I. Kamwa, A. K. Pradhan, and G. Joos, "Adaptive phasor and frequency-tracking schemes for wide-area protection and control," *IEEE Trans. Power Del.*, vol. 26, no. 2, pp. 744–753, Apr. 2011.

[22] P. Kundu and A. K. Pradhan, "Enhanced protection security using the system integrity protection scheme (SIPS)," *IEEE Trans. Power Del.*, vol. 31, no. 1, pp. 228–235, Feb. 2016.

[23] W. D. Stevenson, *Elements of Power System Analysis*, 4th ed. New York, NY, USA: McGraw-Hill, 1982.

[24] Y. Liao and M. Kezunovic, "Online optimal transmission line parameter estimation for relaying applications," *IEEE Trans. Power Del.*, vol. 24, no. 1, pp. 96–102, Jan. 2009.
[25] L. Breiman, J. H. Friedman, and R. A. Olshen, *Classification and Regression Trees*. London, U.K.: Chapman & Hall, 1984.
[26] D. Williams. (May 2008). *Rattle (the R Analytical Tool to Learn Easily), Version 2.3*. [Online]. Available: http://rattle.togaware.com/
[27] *Performing Load Encroachment with an L-PRO*. Accessed: Jun. 22, 2020. [Online]. Available: https://www.erlphase.com/downloads/application_notes/Performing_Load_Encroachment_with_an_LPRO.pdf
[28] M. K. Jena, S. R. Samantaray, and B. K. Panigrahi, "A new adaptive dependability-security approach to enhance wide area back-up protection of transmission system," *IEEE Trans. Smart Grid*, vol. 9, no. 6, pp. 6378–6386, Nov. 2018.
[29] B. Sahoo and S. R. Samantaray, "System integrity protection scheme for enhancing backup protection of transmission lines," *IEEE Syst. J.*, vol. 15, no. 3, pp. 4578–4588, Sep. 2021.
[30] P. K. Nayak, A. K. Pradhan, and P. Bajpai, "Wide-area measurement-based backup protection for power network with series compensation," *IEEE Trans. Power Del.*, vol. 29, no. 4, pp. 1970–1977, Aug. 2014.

BISWAJIT SAHOO (Member, IEEE) received the B.Tech. degree in electrical engineering and the Ph.D. degree from the School of Electrical Sciences, Indian Institute of Technology Bhubaneswar, India, in 2013 and 2021, respectively. His research interests include wide-area measurement-based back-up protection and intelligent protection for transmission systems, including FACTs.

SUBHRANSU RANJAN SAMANTARAY (Senior Member, IEEE) received the B.Tech. degree from UCE Burla and the Ph.D. degree from NIT Rourkela.

He did his postdoctoral studies at McGill University, Canada. He is currently an Associate Professor with the School of Electrical Sciences, Indian Institute of Technology Bhubaneswar, India. His major research interests include PMU and wide area measurement, intelligent protection for transmission systems, including FACTs, micro-grid protection, including distributed generation, micro-grid planning, wide-area-based dynamic security assessment in large power networks, and smart-grid technologies. He is a fellow of the Institution of Engineering and Technology (IET), U.K. He is a member of the IEEE Power Systems Stability Sub-Committee. He has received the prestigious NASI-SCOPUS Young Scientists Awards-2015, the IEEE PES Technical Committee Prize Paper Award-2012, and the Samanta Chandra Sekhar Award, Odisha Bigyana Acadmey-2010. He is an Associate Editor of IEEE Systems Journal and IEEE Transactions on Smart Grid, an Associate Editor (past) of IEEE Transactions on Power Delivery and *IET Generation, Transmission and Distribution*. He is a Guest Editor of IEEE Sensors Journal.

INNOCENT KAMWA (Fellow, IEEE) received the B.S. and Ph.D. degrees in electrical engineering from Laval University, Québec City, in 1985 and 1989, respectively.

He has been a Research Scientist and a Registered Professional Engineer at the Hydro-Quebec Research Institute, since 1988, specializing in system dynamics, power grid control, and electric machines. After leading the System Automation and Control Research and Development Program for years, he became the Chief Scientist for smart grid, the Head of power system and mathematics, and the Acting Scientific Director of IREQ, in 2016. He was an Adjunct professor at Laval University and McGill University. He currently heads the Power Systems Simulation and Evolution Division, overseeing the Hydro-Quebec Network Simulation Centre known worldwide. He became a fellow of IEEE, in 2005, for "innovations in power grid control," and a fellow of the Canadian Academy of Engineering. His honors include the four IEEE Power Engineering Best Paper Prize Awards, the three IEEE Power Engineering Outstanding Working Group Awards, and the 2013 IEEE Power Engineering Society Distinguished Service Award. He is a Co-Editor-in-Chief of *IET Generation, Transmission and Distribution* and an Editor of the *International Journal of Electrical Power and Energy Systems*.